The low-temperature antiferromagnetic structure of Mn_5Si_3 revised in the light of neutron polarimetry*

P J Brown†, J B Forsyth‡, V Nunez† and F Tasset†

† Institut Laue–Langevin, BP 156 38042, Grenoble Cédex, France
‡ Rutherford Appleton Laboratory, Chilton, Oxon OX11 0QX, UK

Abstract. The magnetic structures previously proposed for the low-temperature antiferromagnetic phase (AFI) of the intermetallic compound Mn_5Si_3 have been revised in the light of the results of neutron polarimetry in conjunction with unpolarized-neutron single-crystal integrated-intensity measurements. At 4.2 K the commensurate magnetic unit cell is orthorhombic with $a = 6.889$, $b = 11.901$ and $c = 4.805$ Å and it is related to the hexagonal cell of the paramagnetic phase by $b \approx \sqrt{3}a$. The hexagonal cell contains four Mn1, six Mn2 and six Si atoms. The non-collinear magnetic structure of the AFI phase is stable below 66 K and has monoclinic symmetry. At 4.2 K the Mn1 atoms have moments of $1.20(5)\mu_B$ inclined parallel and antiparallel to the polar direction $\theta = 116(1)°$, $\phi = 105(1)°$, where θ is measured from [001] and ϕ from (010). One third of the Mn2 atoms carry no moment, one third have moments of $2.30(9)\mu_B$ at $\pm[\theta = 70(1)°$, $\phi = 93(1)°]$ and the remainder have $1.85(9)\mu_B$ at $\pm[\theta = 21(1)°$, $\phi = 11(7)°]$. The non-collinearity is attributed to topological frustration and the wide variation in the magnetic moments to the combined effects of Mn moment instability, frustration and single-ion anisotropy.

1. Introduction

Two conflicting magnetic structures [1, 2] have been proposed to describe the long-range antiferromagnetic order in the intermetallic compound Mn_5Si_3. This phase adopts the $D8_8$ structure illustrated in figure 1, with space group $P6_3/mcm$. The unit cell parameters at 300 K are $a = 6.910$, $c = 4.814$ Å with $Z = 2$[3]. The atomic positions [3, 4] are:

Mn1 in 4(d) 32 at $\pm(\frac{1}{3}, \frac{2}{3}, 0; \frac{1}{3}, \frac{2}{3}, \frac{1}{2})$;
Mn2 in 6(g) mm at $\pm(x, 0, \frac{1}{4}; 0, x, \frac{1}{4}; \bar{x}, \bar{x}, \frac{1}{4})$ with $x = 0.2360(1)$;
Si in 6(g) mm at $\pm(x, 0, \frac{1}{4}; 0, x, \frac{1}{4}; \bar{x}, \bar{x}, \frac{1}{4})$ with $x = 5.991(2)$.

The structure of the low-temperature antiferromagnetic phase, AFI, of Mn_5Si_3 at 4.2 K was first studied some 25 years ago by Lander, Brown and Forsyth [1] who used both single-crystal and powder samples. The lowest-angle magnetic reflection is $(\frac{1}{2} \, 0 \, 0)$ and they proposed a structure which was based on an ortho-hexagonal unit cell with $a_o = a_h$; $b_o = \sqrt{3}a_h$; $c_o = c_h$ and moments lying in the (001) plane.
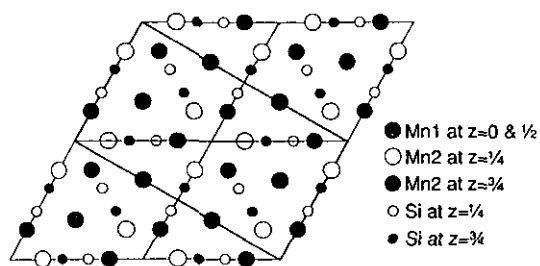
Figure 1. [00.1] projection of the structure of Mn_5Si_3. Four hexagonal unit cells are shown. The orthohexagonal unit cell used to describe the magnetic structure is outlined with bold lines.

● Mn1 at z=0 & ½
○ Mn2 at z=¼
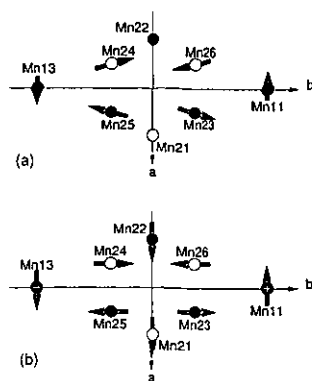● Mn2 at z=¾
○ Si at z=¼
● Si at z=¾

Figure 2. The general motive for the low temperature structure AF1 of Mn_5Si_3 (a) proposed by [1] and (b) proposed by [2]. The signs on the Mn1 atoms indicate the directions of components of moment parallel to c on the atoms at $z = 0$; these components are reversed on the atoms at $z = \frac{1}{2}$.

It gave a reasonable fit to the data (R-factor $\simeq 20\%$), yet had some very unusual features: in particular, the moments on two of the six sub-lattices of Mn2 atoms were zero as illustrated in figure 2(a). This aspect of the structure was determined from the complete absence of magnetic scattering in the ortho-hexagonal $\{h0l\}$ reflections and the fact that the two atoms in question lie on the mirror plane perpendicular to [010] so they cannot be superposed on a symmetrically related but oppositely oriented sublattice in the corresponding [010] projection.

A second, high-temperature, antiferromagnetic phase AF2, stable between 66 K and 99 K, was subsequently identified by Povzner *et al* [5] who proposed a structure, on the basis of neutron-powder diffraction data, in which only the Mn1 atoms are magnetically ordered. There was, however, no obvious relationship between the values of the magnetic moments on the Mn1 sites in this proposed structure for AF2 and those found in the AF1 phase [1]. The existence of the AF2 phase was missed in the original study [1] because the disappearance at 66 K of the ($\frac{1}{2}$ 0 0) magnetic reflection from the powder sample was interpreted as indicating the Néel point. The more extended powder study [5] confirmed this observation, but clearly showed that other magnetic reflections remained until the true Néel point at 99 K.

Recently Menshikov *et al* [2] re-examined the magnetic structures adopted by Mn_5Si_3, using symmetry arguments to identify possible structures and powder diffraction data to choose between them. They also undertook complementary single-crystal measurements which showed that the transitions from paramagnetism to AF2 and from AF2 to AF1 are both of first order and are accompanied by distortions of the orthorhombic a/b axial ratio from the ideal ortho-hexagonal value. The structure they proposed for the low-temperature AF1 phase is very different from that given by [1], the average Mn moment being much larger and the individual moments differently oriented.

These discrepancies have led us to re-examine the absolute scale of the magnetic data presented in [1] and to use the technique of zero-field polarimetry to redetermine the AF1 structure.

Two cross checks lead us to conclude that the magnetic structure factors and magnetic moments quoted in [1] should be scaled up by a factor of $\sqrt{3}$. Firstly, Sheinker *et al* [6] have shown that the magnetic powder lines characteristic of the AF1 structure are present in ternary alloys between Mn_5Si_3 and Mn_5Ge_3 and that their intensities *diminish* monotonically with increasing germanium content, finally disappearing at 50/50 Si/Ge. Recent measurements [7] on a single crystal of $Mn_5(Si_{0.82}Ge_{0.18})_3$ give a structure factor of 1.82×10^{-12} cm per orthohexagonal unit cell for the (010) reflection after scaling to the nuclear intensities, taking into account that all three orthorhombic domains contribute to any nuclear reflection, whereas only one domain contributes to any given magnetic reflection. This value is, however, *greater* than the value of 1.18×10^{-12} cm quoted in [1]. Assuming that the data in [1] were scaled incorrectly and should be $\sqrt{3}$ times larger, gives a value of 2.04×10^{-12} cm for the structure factor of (010) implying a moment reduction in the 18% Ge alloy in fair agreement with the results of Sheinker *et al*. Secondly and perhaps more importantly, the powder data of [2] also give a value $\sim 2 \times 10^{-12}$ cm for the structure factor of (010) thus confirming this rescaling.

The revised moment values for the AF1 structure proposed by [1] and those proposed by [2] are still very different. In the latter structure all the Mn2 atoms carry a moment $(1.1\mu_B)$ and the Mn1 atoms have a very much larger moment of $2.45\mu_B$ compared to $0.69\mu_B$ from the rescaled moments of Lander *et al*: a component of this moment is along [001]. This structure is illustrated in figure 2(*b*). The magnitudes and directions of the magnetic moments on each of the Mn sub-lattices in the AF1 structures of [1] and [2] are given in table 1.

We have already shown [8–10] that the recently developed zero-field neutron polarimeter, CRYOPAD [11], can provide data which depend critically on the moment directions in the scattering sample and are more sensitive to this aspect of the magnetic structure than are integrated intensity measurements. In view of the conflict between the different magnetic structures put forward for Mn_5Si_3, we have used this device to determine the scattered polarization in a number of reflections from a single-crystal sample at 5 K. We now report the results of these measurements which, when combined with the unpolarized beam integrated-intensity measurements, have enabled us to make a better determination of the magnetic structure of the AF1 phase.

2. Definition of axes

In what follows we will use the vectors a, b, c, a^*, b^*, c^* to define the real and reciprocal orthorhombic unit cells of one configuration domain; the axes x, y, z and the reflection indices h, k, l refer to these crytallographic axes. Retaining the convention used in [1] that $b \simeq \sqrt{3}a$, the cell dimensions of the AF1 phase at 4.2 K are $a = 6.889$, $b = 11.901$ and $c = 4.805$ Å [12]. For each reflection measured, another set of axes X, Y, Z are defined with X parallel to the scattering vector, Z vertical and Y making up a right handed set. From its definition, the magnetic interaction vector Q always lies in the YZ plane.

3. Experimental details

No single-crystal material remained from the original study of Mn_5Si_3 [1], but we were able to use a 1 g crystal from an ingot prepared in the Polytechnic Institute,

Table 1. Definition of the labels for the moments on the different Mn sublattices in Mn$_5$Si$_3$ and the coupling schemes between them which have been proposed. The atomic positions and components of the moment are given on the orthohexagonal axes defined in the text. Structure [1] is that of Lander *et al* (1967), structure [2] that of Menshikov *et al* (1990) and the new structure is that proposed in this paper, with the moments increased by a factor of $\sqrt{3}$ (see text).

Atom	Moment vector	Position x	y	z	Structure [1] Coupling scheme x	y	z	Values (μ_B)	Structure [2] Coupling scheme x	y	z	Values (μ_B)	New structure coupling scheme
Mn1	S_{11}	0	$\frac{1}{3}$	0	S_{1x}	0	0	$S_{1x} = 0.7$	S_{1x}	0	$-S_{1x}$	$S_{1x} = 0.9$	S_{11}
	S_{12}	0	$\frac{1}{3}$	$\frac{1}{2}$	S_{1x}	0	0		S_{1x}	0	S_{1x}	$S_{1z} = 2.25$	S_{11}
	S_{13}	0	$\frac{2}{3}$	0	$-S_{1x}$	0	0		$-S_{1x}$	0	S_{1z}		$-S_{11}$
	S_{14}	0	$\frac{2}{3}$	$\frac{1}{2}$	$-S_{1x}$	0	0		$-S_{1x}$	0	$-S_{1z}$		$-S_{11}$
Mn2	S_{21}	$2x$	0	$\frac{1}{4}$	0	0	0	$S_{2x} = 0.5$	S_2	0	0	$S_2 = 1.1$	0
	S_{22}	$\overline{2x}$	0	$\frac{3}{4}$	0	0	0	$S_{2y} = 1.9$	S_2	0	0		0
	S_{23}	x	x	$\frac{3}{4}$	S_{2x}	S_{2y}	0		0	S_2	0		S_{23}
	S_{24}	$\overline{x}$	$\overline{x}$	$\frac{1}{4}$	$-S_{2x}$	S_{2y}	0		0	S_2	0		S_{24}
	S_{25}	x	$\overline{x}$	$\frac{3}{4}$	$-S_{2x}$	$-S_{2y}$	0		0	$-S_2$	0		$-S_{23}$
	S_{26}	$\overline{x}$	x	$\frac{1}{4}$	S_{2x}	$-S_{2y}$	0		0	$-S_2$	0		$-S_{24}$

Ekaterinburg and used by Menshikov *et al* in their neutron studies [2]. This was in the form of a 85° sector, 4 mm in length, cut from a cylindrical sample 15 mm in diameter parallel to its [100] cylinder axis. One rectangular face of the sector was perpendicular to [001] and had dimensions 7×4 mm and the other, almost perpendicular to [010], 6×4 mm.

The crystal was carefully aligned and mounted successively with its [100] and [001] axes vertical in the zero-field polarimeter CRYOPAD on the IN20 polarized-beam triple-axis spectrometer at the Institut Laue–Langevin, Grenoble. The analyser and detector both move in the horizontal plane, so these crystal mountings allowed $\{0kl\}$ and $\{hk0\}$ reflections to be measured, respectively.

The principles and operation of the CRYOPAD have been fully described elsewhere by Brown *et al* [8] and by Tasset [11]. In short, it allows both the input neutron-beam polarization to be set to any desired angle and the magnitude and direction of the polarization in a diffracted beam to be found under computer control. The diffracting sample is kept in a field-free region and its temperature can be maintained in the range 2–315 K. The measurements on the AF1 phase were made at 5 K and the Heusler alloy monochromator and analyser crystals of IN20 were set to a wavelength of 1.532 Å. Although the CRYOPAD makes it possible to set the input polarization P to any desired angle, it is convenient from the point of view of subsequent analysis to make scans in which P is varied in the three principal planes defined by the axes X, Y and Z. In view of the time available, the present measurements were restricted to the six 'cardinal directions' parallel to $\pm X$, $\pm Y$ and $\pm Z$. The most significant feature of the results was that the scattered polarization was found always to be closely parallel or antiparallel to the incident polarization. Its magnitude was maintained for incident polarization parallel to the scattering vector (X) but reduced to a greater or lesser extent when parallel to the Y or Z directions. The scattered polarizations measured with the incident polarization parallel to Y and Z for a few key reflections are given in table 2. A complete list of the results can be found in table 5.

Table 2. Polarization scattered parallel to the incident polarization for incident directions parallel to $Y(P_Y)$ and $Z(P_Z)$, for some key reflections measured with [100] parallel to Z.

hkl	P_Y	P_Z
010	0.46	−0.46
030	0.35	−0.33
050	0.39	−0.35
011	0.89	−0.90
031	0.91	−0.92
051	0.91	−0.87
032	0.65	−0.65

4. Qualitative constraints on possible structures

The results of the polarimetry measurements could not be understood in terms of either of the two structures already proposed. We have therefore first determined the qualitative features which the scattered polarizations impose on the magnetic

structure. This qualitative structure is then used as the starting point for a structure refinement based on both polarization and integrated-intensity measurements.

The most important property of the scattered polarizations which imposed qualitative constraints on possible magnetic structures is the fact, noted above, that there is no rotation of the scattered polarization when the incident polarization is along any of the cardinal directions X, Y, Z. The only effect of the magnetic scattering process on the polarization is to reduce its magnitude to a greater or lesser extent and possibly to reverse its direction.

In the purely magnetic reflections characteristic of an antiferromagnetic structure such as that of Mn_5Si_3, which has a non-zero propagation vector, depolarization can only occur because of the existence of more than one type of antiferromagnetic domain. This itself implies that the magnetic symmetry must be less than the configurational symmetry. The polarization scattered by a pure magnetic reflection with interaction vector Q for an incident polarization P is:

$$\{2\,\mathrm{Re}[Q(P \cdot Q^*)] - PQ \cdot Q^*\}/(Q \cdot Q^*).$$

This corresponds to precession of the incident polarization direction around the direction of Q by 180° without change in its magnitude [13]. If more than one domain is present in the crystal the final polarization is the sum of the polarizations scattered by each domain, weighted by the intensity scattered by that domain (equal to $\alpha_i Q_i \cdot Q_i^*$ where α_i is the domain population) and normalized by the total scattered intensity. For incident polarizations in the cardinal directions X, Y, Z the scattered polarization will only be systematically parallel or antiparallel to the incident direction if the domains are equally populated and the Q for the different domains are related by symmetry into pairs of equal magnitude, oriented so that the directions Y and Z bisect the angles between them. Under these conditions, as illustrated in figure 3, the components of scattered polarization perpendicular to P are equal in magnitude and opposite in direction for the two members of a pair and the resultant scattered polarization is given by:

$$\sum_j \cos(2\phi_j)|Q_j|^2 / \sum_j |Q_j|^2$$

where ϕ_j is the angle between P and Q_j for a symmetric pair of domains, and the sum is over all such pairs.

In Mn_5Si_3 the configurational symmetry is orthorhombic, mmm, but this holosymmetry can only be preserved in the antiferromagnetic structure if the spins are aligned along one of the axes of the orthorhombic cell. In the structure proposed in [1] there are components of spin along both a and b. The only true symmetry elements of the magnetic symmetry are the glide plane perpendicular to a at $x = 0$, and the mirror plane perpendicular to c passing through the Mn2 atoms; neither of these elements is combined with time reversal. The mirror plane perpendicular to b, which is not retained in the magnetic structure, relates the two types of magnetic domain in this case. The magnetic structure factors $M(\kappa)$ for the two domains are linked by the identities:

$$M(\kappa)_1 \cdot a = M(\kappa)_2 \cdot a \qquad M(\kappa)_1 \cdot b = -M(\kappa)_2 \cdot b \qquad M(\kappa)_1 \cdot c = M(\kappa)_2 \cdot c = 0.$$

For the $0k0$ reflections measured with [100] vertical the scattered polarization is $\simeq 0.35$ and is flipped for P parallel to Z, indicating an angle ϕ between Q and Z of $\simeq 65°$. This result shows that the assumption of no moment parallel to c cannot
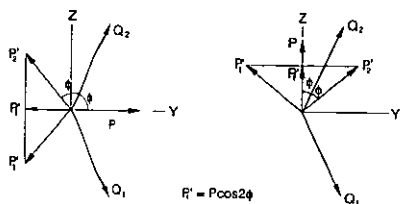
Figure 3. The rotation of the polarization direction by scattering from two symmetrically related magnetic domains with magnetic interaction vectors Q_1 and Q_2. The incident polarization P is rotated to P_1' by Q_1 and P_2' by Q_2. The resultant scattered polarization P_f' is $P \cos 2\phi$ where ϕ is the angle between P and Q. (a) P parallel to Y. (b) P parallel to Z.
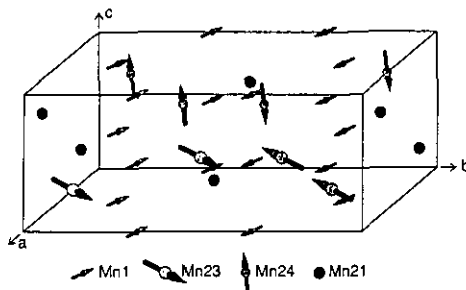
Figure 4. Schematic representation of the new magnetic structure proposed for Mn₅Si₃ below 66 K. The size of the arrows is proportional to the magnitude of the moments at 4.2 K.

be correct, since such components provide the only contribution to Q_Y in these $0k0$ reflections.

To proceed further it is helpful to write down the general form of the magnetic structure factors for the class of magnetic structures which maintain antiparallelism between atoms related by the mirror plane perpendicular to b (it is only this class of structures which give no magnetic reflections of the form $h0l$). For Mn1 the independent moments as defined in table 1 are:

$$S_{11}\text{on Mn11 at } 0, \tfrac{1}{3}, 0 \qquad S_{12}\text{on Mn12 at } 0, \tfrac{1}{3}, \tfrac{1}{2}$$

and the magnetic structure factor is

$$4f_{\mathrm{Mn}}(S_{11} \pm S_{12})\sin 2\pi(k/3).$$

For Mn2 the moments are

$$S_{23}\text{on Mn23 at } x, x, \tfrac{1}{4} \qquad S_{24}\text{on Mn24 at } \bar{x}, \bar{x}, \tfrac{3}{4} \text{ with } x = 0.88015$$

and the structure factor is

$$-2(\mathrm{i})^l f_{\mathrm{Mn}}[(\pm S_{23} + S_{24})\sin 2\pi hx + \mathrm{i}(-S_{23} \pm S_{24})\cos 2\pi hx)]\sin 2\pi kx.$$

In both structure factor expressions, the $+$ sign applies to reflections with l even and the minus sign to those with l odd. It is apparent that Mn1 does not contribute to reflections with $k = 3n$. For the reflections 030 and 032 the geometric parts of the magnetic structure factors are the same and depend on $S_{23} - S_{24}$. From the discussion of the $0k0$ reflections given previously, we deduce that this difference must have components parallel to both a and c. The fact that the polarization scattered by the 032 reflection is greater than that scattered by the 030 reflection and, like it, is flipped for P parallel to a shows that there must in addition be a component of $S_{23} - S_{24}$ parallel to b.

In contrast to the $0kl$ reflections with l even, those with l odd scatter with little depolarization. The observation that they also flip the incident polarization when it is parallel to a shows that the component parallel to a of both $S_{11} - S_{12}$ and $S_{23} + S_{24}$ must be small. These reflections are, on the other hand, quite strong which indicates

that at least one and probably both of the other two components must be finite. There can therefore be no simple relationship between the moments S_{23} and S_{24} which are on atoms related by the centre of symmetry at the origin. The magnetic structure is therefore non-centrosymmetric and the atoms Mn23 and Mn24 will be treated as magnetically independent. Assuming initially that the magnitudes of the moments on these two atoms are equal, the constraints imposed by the scattered polarizations observed for the 030, 031 and 032 reflections can be satisfied by orientations of S_{23} and S_{24} given by the polar coordinates: $\theta_{23} \simeq 76°$, $\phi_{23} \simeq 45°$; $\theta_{24} \simeq 14°$, $\phi_{24} \simeq 45°$. For the group of reflections 010, 030 and 050 it can be seen in table 2 that the scattered polarizations are very similar. It can thus be inferred that the projection on 101 of the vector $S_{11} + S_{12}$ which contributes to 010 and 050 but not to 030, must be nearly parallel or antiparallel to that of $S_{23} - S_{24}$, which contributes to all three. The fact that both the 010 and 050 reflections are more intense than 030 shows that they are antiparallel since the geometric parts of the structure factors have opposite signs. Making the hypothesis that $S_{11} = S_{12}$, the orientation of S_{11} must be approximately given by $\theta_{11} \sim 145°$, $\phi_{11} \sim 180°$.

5. Refinement of the magnetic structure

The magnetic structure determination [1] indicated Mn moments around $1\mu_B$ so this magnitude was taken as a starting value for both moments. Since the polarization values are relatively insensitive to the magnitudes of the moments, a preliminary refinement was carried out using the integrated intensity data of [1] to test its consistency with the orientations determined above and to obtain improved values for the magnetic moments. The result of this refinement is given in column 3 of table 3. The parameters obtained from the intensity-based refinement were used as starting values for one based on the scattered polarizations, whose results are given in column 4 of table 3. The orientations of the moments are not changed significantly, but, as expected, are determined more precisely by the scattered polarizations. On the other hand, the ratio between the Mn1 and Mn2 moments determined from the two refinements is significantly different. To resolve this problem it was found necessary to allow the vectors S_{23} and S_{24}, which already have different orientations, to have different magnitudes. This allowed a final set of parameters to be obtained which are consistent with both the integrated intensities and the scattered polarizations. These are given in column 5 of table 3. The comparison between observed and calculated magnetic-structure amplitudes is given in table 4 and that between the observed and calculated polarizations in table 5. It can be seen that excellent agreement has been obtained.

6. Discussion

The structure obtained above for the low-temperature antiferromagnetic phase of Mn_5Si_3 has monoclinic symmetry and is illustrated schematically in figure 4. It is, perhaps surprisingly, rather complex and contains a variety of different Mn moments arranged in a highly non-collinear manner. On the other hand, it is well known that the Mn moment in metallic systems exhibits instability [14] and that its magnitude, in compounds with the B-group metalloids, depends strongly on its environment [15]. The non-collinearity of the Mn2 moments and the absence of moment on one third of

Table 3. Parameters obtained at different stages in the refinement of the low-temperature magnetic structure of Mn_5Si_3. $R(F)$ is the agreement factor for magnetic structure factors:

$$\left(\sum |F_{obs} - F_{calc}|\right) \times 100 / \sum F_{obs}$$

$$\chi^2 = \sum [(Q_{obs} - Q_{calc})/\sigma(Q_{obs})]^2 / (n_{obs} - n_p)$$

where the Q are the structure factors for $\chi^2(F)$ and the components of scattered polarization for $\chi^2(P)$; n_{obs} is the number of observations and n_p the number of parameters refined in each case.

Parameter	Initial estimate	Refinement using:		
		structure factors	scattered polarization	combined
$S_{11}\,\mu\,(\mu_B)$	1.0	1.35(9)	1.35	1.20(5)
$\theta(°)$	145	107(9)	116(1)	116(1)
$\phi(°)$	180	117(7)	105(1)	105(1)
$S_{23}\,\mu\,(\mu_B)$	1.0	2.1(5)	1.8(1)	2.30(9)
$\theta(°)$	76	72(5)	72(2)	70(1)
$\phi(°)$	45	82(14)	96(1)	93(1)
$S_{24}\,\mu\,(\mu_B)$	1.0	2.1(5)	1.8(1)	1.85(9)
$\theta(°)$	14	18(8)	22(1)	21(1)
$\phi(°)$	45	14(21)	2(5)	11(7)
$R(F)\,(\%)$	30	7	14	6.5
$\chi^2(F)$	122	5.5	19	4.1
$\chi^2(P)$	131	34	5.3	4.7

them may be interpreted as a response to frustration in the puckered ring of six Mn2 atoms. If there were antiferromagnetic interactions both between neighbours in the ring and between members of the coplanar triangles (see figure 5), and all exchange interactions in the ring were equal and proportional to $S_i \cdot S_j$, then the optimum arrangement would be the triangular one of figure 5(a). The arrangement found, which is idealized in figure 5(b), can be favoured if the exchange within the plane triangles (interatomic distance 2.85 Å) is stronger than that between neighbours in the ring (distance 2.92 Å), as this coupling scheme also reduces the frustration at the Mn1 site as shown in figure 6. The change from hexagonal to orthorhombic symmetry implicit in this latter arrangement allows the interatomic vector associated with the strong antiferromagnetic Mn2–Mn2 interaction to be optimized independently of the other two edges of the triangle which link magnetic and non-magnetic Mn2 atoms. The orthorhombic cell measured by [12] at 5 K gives Mn23–Mn25 = 2.853 Å compared to 2.859 for Mn23–Mn22.

The Mn1–Mn2 interactions (interatomic distance 2.93 Å) must be ferromagnetic as the direction of the moment on the Mn1 atoms is approximately parallel to the vector sum of the moments on their four Mn2 neighbours. Thus the changeover from ferromagnetic to antiferromagnetic interactions in this compound occurs at an interatomic distance of about 2.9 Å.

The low moment ($1.20\mu_B$) found for Mn1 is probably due to the close proximity of its two Mn1 neighbours (2.4 Å), since such small distances between Mn atoms are known to lead to instability of the moment [15]. The lack of an ordered moment

Table 4. Comparison between the observed and calculated structure amplitudes for the different models which have been proposed for the low-temperature magnetic structure of Mn_5Si_3. Structure [1] is that of Lander *et al* (1967) and the observed structure factors are taken from that paper and have been multiplied by $\sqrt{3}$ (see text), structure [2] is that of Menshikov *et al* (1990). The new structure is the one proposed in this paper. The uncertainty in the observed structure factors is $\sim 5 \times 10^{-14}$ cm.

		Magnetic structure amplitudes (10^{-14} cm)			
			Calculated		
hkl	$(\sin\theta/\lambda$ $(\text{\AA}^{-1})$	Observed	[1]	[2]	New
010	0.0420	204	201	204	195
100	0.0726	0	0	0	0
120	0.1110	197	159	141	189
011	0.1122	154	223	189	151
030	0.1260	87	74	99	88
101	0.1269	0	0	81	0
210	0.1511	258	208	149	258
121	0.1522	204	201	265	199
031	0.1634	165	154	89	159
140	0.1831	118	94	110	109
211	0.1835	126	36	243	111
230	0.1922	178	165	147	177
050	0.2101	121	118	130	113
102	0.2204	0	0	0	0
320	0.2334	256	177	111	253
051	0.2344	85	55	216	83
122	0.2359	225	184	123	225
032	0.2433	73	48	64	91
250	0.2553	92	85	73	118
212	0.2572	159	147	121	140
160	0.2623	87	52	26	105
340	0.2750	71	40	53	79
071	0.3120	90	47	155	93
013	0.3150	55	102	63	65
430	0.3165	59	24	5	69
270	0.3280	106	68	54	102
360	0.3331	88	71	32	91
033	0.3367	66	100	58	68
180	0.3439	52	50	54	53
072	0.3603	73	66	60	87
520	0.3724	114	59	37	123
303	0.3806	0	0	24	0
470	0.4132	52	35	33	72

on the Mn21 and Mn22 atoms on the other hand is the direct result of frustration, the topology of the magnetic structure gives an identically zero internal field at these sites. The difference between the magnitude of the moments on Mn23 and Mn24 must arise from the fact that their magnetic moments have different orientations with respect to the local environment. This could arise from a kind of single-ion anisotropy induced by the crystal field due to the coordinating Si atoms.

7. Conclusions

The antiferromagnetic structure adopted by Mn_5Si_3 at temperatures below 66 K has

Table 5. Comparison between the components of polarization scattered parallel to the incident polarization by magnetic reflections of Mn$_5$Si$_3$ at 5 K and those calculated from the magnetic structure proposed here. The observed scattered polarizations have been normalized by dividing by the estimated value of the incident polarization. The X, Y and Z axes are defined with X parallel to the scattering vector, Z perpendicular to plane of the incident and scattered beams and Y making up an orthogonal right-handed set. The hkl are given on the orthohexagonal axes and were measured with [100] parallel to Z for the first group and [001] parallel to Z for the second group. Aberrations of the polarimeter limit the accuracy of measurement of the scattered polarizations to $\simeq 0.03$.

| hkl	P_X obs.	P_X calc.	P_Y obs.	P_Y calc.	P_Z obs.	P_Z calc.
010	−0.95	−1.00	0.46	0.42	−0.46	−0.42
011	−0.94	−1.00	0.89	0.90	−0.90	−0.90
030	−0.97	−1.00	0.35	0.22	−0.33	−0.22
031	−0.97	−1.00	0.91	0.91	−0.92	−0.91
032	−0.99	−1.00	0.65	0.74	−0.65	−0.74
051	−0.93	−1.00	0.85	0.91	−0.87	−0.91
050	−0.99	−1.00	0.39	0.43	−0.35	−0.43
071	−0.96	−1.00	0.90	0.91	−0.93	−0.91
320	−1.01	−1.00	0.27	0.31	−0.27	−0.31
210	−1.00	−1.00	0.21	0.19	−0.20	−0.19
120	−0.98	−1.00	−0.44	−0.43	0.44	0.43
230	−0.94	−1.00	−0.36	−0.32	0.37	0.32
160	−0.91	−1.00	−0.69	−0.63	0.64	0.63
250	−1.00	−1.00	−0.15	−0.21	0.17	0.21
140	−0.91	−1.00	−0.10	−0.09	0.11	0.09
320	−1.01	−1.00	0.32	0.31	−0.32	−0.31
010	−0.97	−1.00	−0.42	−0.42	0.42	0.42
030	−0.69	−1.00	−0.17	−0.22	−0.08	0.22
050	−0.96	−1.00	−0.44	−0.43	0.47	0.43
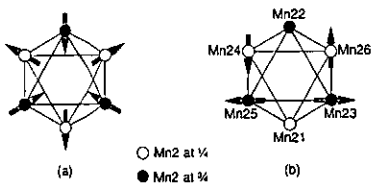
Figure 5. Possible arrangements of spins in a puckered hexagonal ring. (*a*) A triangular pattern giving $\sum S_i \cdot S_j = 6S^2$ if all interactions are equal. (*b*) The relative moment directions found in the actual structure with $\sum S_i \cdot S_j = 2S^2$. For clarity all directions are shown in the plane of the paper (the actual direction of S_{24} is nearly perpendicular to this plane.
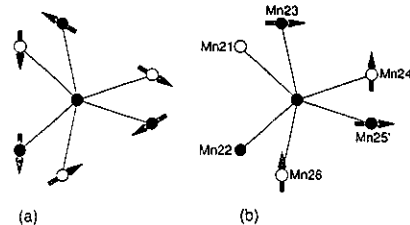
Figure 6. Relative moment directions on the six Mn2 neighbours of an Mn1 atom for: (*a*) the triangular arrangement of figure 5(*a*); (*b*) the actual arrangement with moment directions shown as in figure 5(*b*). For an Mn1 atom at $z = 0$, the black Mn2 atoms are at height $z = -\frac{1}{4}$ and the open Mn2 atoms are at $z = \frac{1}{4}$ as in figure 1. Those atoms whose labels are primed have their moments reversed owing to the periodicity of the magnetic structure.

been redetermined by combining new results of neutron polarimetry with the older magnetic structure factor measurements [1] which have been rescaled to take proper

account of the domain structure. The polarimetric results show that the structure is more complex than that proposed by [1] and in particular that there must be components of moment parallel to *c* as proposed in [2]. On the other hand neither the equality of the Mn2 moments imposed in the structure of Menshikov *et al* [2], nor the large value of $2.45\mu_B$ which they placed on the Mn1 atom can be maintained.

The fact that such a complex structure can be proposed with confidence is due in large part to the strong constraints placed on the magnetic moment directions by the results of neutron polarimetry. Indeed, it is possible to find almost equally good agreement between the observed single-crystal intensity data and those calculated for a structure in which the manganese moments are confined to the (100) plane; however, this constraint is completely at variance with results from polarization analysis. It is therefore not surprising that Menshikov *et al* [2], working with powder data of limited resolution and extent, could obtain a reasonable fit with a structure even more different from our new model. Although the structure factors for the two models are very different (table 4), the effect on the powder pattern is mostly a redistribution of intensity between reflections contributing to overlapping lines.

While complex, our new structure can be understood in terms of the physics already used to describe other antiferromagnetic intermetallic compounds containing manganese [16]. The non-collinearity is due to topological frustration and the wide variation in the magnetic moments to the combined effects of Mn moment instability, frustration and single-ion anisotropy.

Acknowledgments

References

[1]   Lander G H, Brown P J and Forsyth J B 1967 *Proc. Phys. Soc.* **91** 332
[2]   Menshikov A Z, Vokhmyanin A P and Dorofeev Yu A 1990 *Phys. Status Solidi* b **158** 319
[3]   Aronnson B 1960 *Acta. Chem. Scand.* **14** 1414
[4]   Lander G H and Brown P J 1967 *Phil. Mag.* **16** 521
[5]   Povzner A A, Sheinker M E, Krentsis R P and Gel'd P V 1978 *Izv. Vuzov. Fiz.* **5** 126 (Engl. Transl. 1978 *Sov. Phys. J.* **21** 654)
[6]   Sheinker M E, Krentis R P and Gel'd P V 1977 *Sov. Phys.–Solid State* **19** 1109
[7]   Forsyth J B, Brown P J, Matos Beja A M and Alte da Veiga L M 1992 private communication
[8]   Brown P J, Chattopadhyay T, Forsyth J B, Nunez V and Tasset F 1991 *J. Phys.: Condens. Matter* **3** 4281
[9]   Nunez V, Brown P J, Forsyth J B and Tasset F 1991 *Physica* B **174** 60
[10] Nunez V, Brown P J, Chattopadhyay T, Forsyth J B and Tasset F 1992 *Physica* B **180 & 181** 903
[11] Tasset F 1989 *Physica* B **156–157** 627
[12] Istomina Z A, Andreeva L P, Zadvorkin S M and Andreev A V 1983 *Fizicheskie Svoistva Metallov i Splavov* (Sverdlovsk: Ural Polytechnic Institute) p 13
[13] Izyumov Yu A and Maleev S V 1962 *Sov. Phys.–JETP* **14** 1168
[14] Shiga M 1988 *Physica* B **149** 293
[15] Forsyth J B and Brown P J 1990 *J. Phys.: Condens. Matter* **2** 2713
[16] Ballou R, Lacroix C and Nunez-Regueiro M D 1991 *Phys. Rev. Lett.* **66** 1910